2010

Infrared Spectroelectrochemical Reduction of Iron Porphyrin Complexes

Zhongcheng Wei
Marquette University

Michael D. Ryan
Marquette University, michael.ryan@marquette.edu

Inorganic Chemistry, Vol. 49, No. 15 (July 6, 2010): 6948-6954. DOI.

Infrared Spectroelectrochemical Reduction of Iron Porphyrin Complexes

Zhongcheng Wei
Chemistry Department, Marquette University, Milwaukee, Wisconsin
Michael D. Ryan
Chemistry Department, Marquette University, Milwaukee, Wisconsin

SUBJECTS:
Carbonyls, Iron, Nitrosyls, Pyrroles, Redox reactions

Abstract

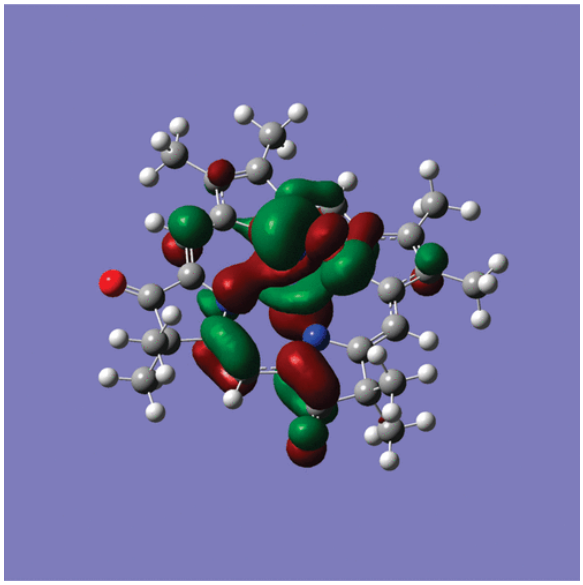

The spectroelectrochemistry of iron porphinones and their nitrosyl complexes were examined by infrared spectroscopy, as well as ferrous octaethylporphyrin nitrosyl. With the use of d_8-THF, the solvent was transparent down to 1200 cm^{-1}. For the porphinones, the reduction of the macrocycle ring could be observed by the changes in the ν_{CO} band and, for the nitrosyl complex, the changes in the nitrosyl ligand were directly observable from the ν_{NO} band. Formation of the ferrous complexes led to a small downshift in the ν_{CO} band. Further reduction to the formal Fe("I") complex led to more complex spectra which were interpreted with the help of density functional theory (DFT) calculations. The reduction of Fe(OEP)(NO) and its porphinone analogues was also examined. The reduction of the iron porphyrin and porphinone nitrosyl complexes lead to substantial decreases in the ν_{NO} band from 1665 to 1670 cm^{-1} to 1442–3 cm^{-1}. The energy of the ν_{NO} band in the reduced complex was unaffected by the presence of carbonyl groups on the porphinone ring, indicating little additional delocalization of the electron density of the Fe-NO moiety because of the carbonyl groups. The identity of the ν_{NO} bands was confirmed with ^{15}N substitution of the Fe(OEP)(NO) complex. The ν_{CO} band on the porphinone ring was found to be sensitive to the degree than electron density was delocalized to the ring.

Synopsis

The infrared spectroelectrochemistry of iron nitrosyl porphyrins and porphinones was examined. The most prominent features of the spectra were the nitrosyl and carbonyl bands which were sensitive to the oxidation state of the complex. The identity of the nitrosyl bands in the starting and reduced material was confirmed by ^{15}N substitution in the nitrosyl group. DFT calculations were used to help understand the spectral changes.

Introduction

The electrochemical reduction of iron porphyrins and their nitrosyl complexes is quite interesting and intriguing because the metal, porphyrin, and NO group are all capable of accepting electrons. For example, the reduction of the ferrous complex to the formal Fe(I) state has been quite controversial with both the iron(I) porphyrin and the iron(II) porphyrin radical anion being proposed as products. Because of electron delocalization, neither structure accurately represents the true electronic structure. With that in mind though, the predominant electronic structure of the $Fe(P)^-$ species is strongly influenced by the identity of the porphyrin ring. For example, Yamaguchi and Morishima (1) were able to change the electronic structure from an iron(I) porphyrin to

an iron(II) π -anion radical by changing the β-pyrrole substituents. Donohue et al. (2) had earlier observed the same transitions with tetraphenylporphyrins, using resonance Raman spectroscopy.

Less studied with regard to iron(II) reduction have been the porphinones and porphinediones (see Scheme 1). The porphinedione structure has been shown to be present in heme d_1, the active site of heme-containing dissimilatory nitrite reductases. The electrochemistry and spectroelectrochemistry of iron porphinones and their nitrosyl complexes have been reported. (3, 4) In general, the electrochemical properties of the porphinone complexes have been quite similar to their porphyrin analogues. The presence of the ketone group(s) on the ring lowered the $E_{1/2}$ of the ferric/ferrous reduction of octaethylporphinone (FeOEPone) and octaethylporphinedione (FeOEPdione) by 100 and 290 mV, respectively. (4, 5) By contrast, the $E_{1/2}$ for the formal Fe(II)/Fe(I) decreased by only 30 and 110 mV, respectively. (4) The $E_{1/2}$ values for the reduction of the nitrosyl complexes of iron porphinones have been previously reported. (6) Reduction of Fe^{II}(P)(NO), where P = OEPone or OEPdione, led to a decrease in the $E_{1/2}$ by 210 and 270 mV, respectively. The electronic state of the reduced complex, where P = porphine, has been the subject of several density functional theory (DFT) studies. (7, 8)

Scheme 1

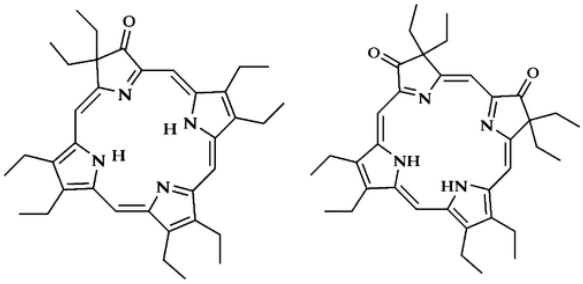

Octaethylporphinone (OEPone) Octaethylporphinedione (OEPdione)

Infrared spectroelectrochemistry is ideally suited to investigate the structure of porphinone complexes because of the presence of a ketone group on the macrocyclic ring. The ν_{CO} band in the infrared is significantly stronger than most of the porphyrin ring vibrations, making it easy to observe spectroscopically. The application of infrared spectroelectrochemistry to the study of electrochemical processes has grown dramatically in recent years, especially in the area of metal porphyrin electrochemistry. The ability to obtain structural information on the redox intermediates is an important impetus for this work, even though work in this region of the spectrum is more difficult experimentally than in the visible region. Studies on the changes in CO and NO vibrational frequencies because of oxidation and/or reduction of the metal center (9-12) are particularly attractive because this region is generally clear of overlapping bands. In spite of the experimental difficulties, other workers have investigated the porphyrin vibrations, (13-16) but this area has not been significantly exploited.

The infrared spectra of metalloporphyrins have been studied in considerable detail, (17-20) including the normal-mode analysis of nickel octaethylporphyrin. This has been extended to nickel octaethylchlorin by Prendergast and Spiro. (21) The infrared spectra of porphinediones were examined by Mylrajan et al. (22) Infrared spectroelectrochemistry was used by Zheng et al. (16) to examine the intermediates generated from the reaction of Co(I)TPP^- with alkyl chlorides. Kini et al. (23) monitored the NO vibration in the oxidation of phenyl-substituted Co(TPP)(NO) complexes. In addition to model compounds, the infrared spectroelectrochemistry of cytochrome c in aqueous media has been examined. (24)

The electrochemistry of iron porphyrins in THF shows three one-electron reduction waves:

$$Fe^{III}(P)(Cl) + e^- \rightarrow Fe^{II}(P) + Cl^-$$

(1)

$$\mathrm{Fe^{II}(P) + e^- \rightarrow Fe^{II}(P)^-}$$

(2)

$$\mathrm{Fe(P)^- + e^- \rightarrow Fe(P)^{2-}}$$

(3)

The visible spectroelectrochemistry and the $E_{1/2}$ values for all three waves of Fe^{III}(OEPone)Cl and Fe^{III}(OEPdione)Cl have already been reported, and are summarized in Table 1. (4) The first reduction product is a ferrous compound, followed by the formation of a formal $Fe^{I}(P)^-$ complex. The $Fe^{I}(OEP)^-$ and $Fe^{I}(TPP)^-$ complexes have been studied most extensively by visible, (25) X-ray, (26) NMR, (27) resonance Raman, and electron paramagnetic resonance (EPR) (25) spectroscopy. These complexes are characterized as Fe^{I} complexes with some delocalization to the ring. Little work has been done on the porphinone complexes. Previous work in our laboratory has studied the visible spectra of the products of the reduction of Fe(OEPone)Cl and Fe(OEPdione)Cl complexes. (4) Because it is not possible to characterize the electronic structure of porphyrin species solely on the basis of visible spectra, the infrared spectroelectrochemistry of these compounds was performed.

Table 1. Half-Wave Potentials for Iron Porphinones and Related Nitrosyl Complexes[a]

complex	solvent	$Fe(P)(NO)/Fe(P)(NO)^-$	$Fe^{III}(P)/Fe^{II}(P)$	$Fe^{II}P/Fe^{I}P$	ref.
Fe(OEPone)Cl	THF		−0.35 V	−1.23 V	4
Fe(OEPdione)Cl	THF		−0.16 V	−1.15 V	4
Fe(OEP)(NO)	THF	−1.07 V			6
Fe(OEPone)(NO)	THF	−0.86 V			6
Fe(OEPdione)(NO)	THF	−0.80 V			6

[a]All potentials vs $Ag/AgNO^3$ reference electrode.

The reduction of iron porphyrin-nitrosyl complexes was also studied in this work. These complexes are reduced by one-electron reversible processes. Infrared spectroelectrochemistry was used to monitor the changes in the axial ligand (NO), the ring CO bond (if present) and porphyrin vibrations to obtain information on the effect of reduction on iron porphyrin nitrosyl complexes. This technique is especially attractive for the study of porphinones complexes in that the carbonyl band of the porphinones is quite strong and can be readily observed. Previous work in this laboratory has studied the resonance Raman spectroelectrochemistry of Fe(TPP)(NO). (28) The ν_{NO} could be observed for both the starting material and the one-electron reduced product, but the resonance enhancement of that band in $Fe(TPP)(NO)^-$ was quite low. Lehnert et al. (8) carried out DFT calculations on a number of six-coordinate Fe(porphine)-NO complexes and their one-electron reduced products. The calculations showed that the one electron reduction of Fe(P)(NO)(L) led to double occupation of the singly occupied molecular orbital (SOMO), strengthening the Fe−NO σ-bond, and weakening the N−O vibration. Further studies of $Fe(P)(NO)^-$ were carried out by Pellegrino et al., (7) where P = octabromo-tetrakis-(pentafluorophenyl)porphyrin) ($TFPPBr_6$). Pellegrino et al. obtained visible and infrared spectra of $Fe(P)(NO)^-$ as well as characterization of the bonding by DFT calculations. Their description of $Fe(TFPPBr_6)(NO)^-$ indicated that the actual electronic structure was intermediate between $Fe^{II}NO^-$ and $Fe^{I}NO$, in agreement with Lehnert el al. (8)

Experimental Section

Chemicals

Octaethylporphyrin iron(III) chloride (FeOEPCl) was obtained from Aldrich Chemical Co. Tetrahydrofuran (THF, Sigma Aldrich Chemical Co.), and THF-d_8 was doubly distilled from potassium by heating at reflux temperatures

under an argon atmosphere until the blue benzophenone anion radical was persistent, and then was stored in a glovebox. The porphinones derivatives, (29, 30) the iron complexes, (31) and the nitrosyl complexes (and their ^{15}NO analogues) (6) were synthesized by literature methods. Tetrabutylammonium perchlorate (TBAP, GFS Chemical Co.) was dried under a vacuum at 70 °C for 40 h. ***Caution!*** *While we have had no problems drying TBAP, precautions should be taken in the heating of any perchlorate salt.*

Equipment

Cyclic voltammograms were obtained with a Model CySy2Ra Computer-Controlled Electroanalytical System (Version 7.0 software), Cypress Systems, Inc. A three-electrode cell was used for voltammetric measurements, consisting of a platinum wire working electrode, a platinum flag auxiliary electrode, and an Ag/0.1 M $AgNO_3$ in acetonitrile reference electrode. The reference electrode was separated from the test solution by a salt bridge filled with the appropriate solvent and supporting electrolyte.

The UV−visible spectra were recorded on a HP 8452A diode array spectrophotometer or a Perkin-Elmer 320 UV−visible spectrophotometer. An optically transparent thin layer electrochemical (OTTLE) cell was used for UV−visible spectroelectrochemical experiments. (32) The infrared spectra were obtained on a 4020 Galaxy Series FT-IR spectrometer, Matson Instruments. Prior to obtaining the spectroelectrochemical data, the cell was filled with solvent and electrolyte. This spectrum was then subtracted from all subsequent spectra to obtain the spectra of the iron porphyrin species. The IR OTTLE (33) cell was a modified Wilmad semipermanent cell. A Teflon spacer between two KBr windows was replaced by a polyethylene spacer in which the working, auxiliary and reference electrodes were melt-sealed. The working and auxiliary electrodes were fabricated from 100 mesh platinum gauzes (Aldrich), and a silver wire (diameter 0.05 mm, Johnson Matthey, U.K.) was used as pseudo reference electrode. The entrance window of the cell was masked so that the spectral beam passed only through the working electrode.

Computation

Reported calculations were carried out using the BP86 DFT functional and the TZVP basis set for all elements except iron using the Gaussian 03 suite of programs for electronic structure and vibrational spectral calculations. (34) The Wachters' basis set was used for iron. (35) All calculations converged using the tight optimization criteria.

Procedures

The cyclic voltammetric experiments were carried out in the glovebox. For the spectroelectrochemical measurements, all solutions were prepared and filled into an OTTLE cell in the glovebox. The spectroelectrochemical data were obtained after the current had decayed to the background or become stable.

Results and Discussion

Infrared Spectroelectrochemistry of Ferric Porphinones

While the electrochemistry of iron porphyrins is quite facile in THF, the limited spectral window available for THF in the infrared (mostly opaque below 1500 cm^{-1}) limits its suitability to study iron porphyrins. To increase the spectral window, d_8-THF was used in most of this work, widening the spectral window down to 1200 cm^{-1}. For bands below 800 cm^{-1}, normal abundance THF was more transparent with a window between 300 and 800 cm^{-1}, except for 2 bands due to THF which eliminate the region between 600 and 700 cm^{-1}. For d_8-THF, the transparent region is between 300 and 600 cm^{-1}, but the band around 650 cm^{-1} is weaker in d_8-THF than in normal abundance THF. The prominent bands of Fe(OEPone)Cl can be clearly seen in both the KBr pellet and the THF-d_8 (solvent subtracted). The carbonyl vibration at 1719 cm^{-1} can be observed in both spectra, along with the ethyl bands around 1470 cm^{-1}. Additional porphyrin bands at 1563, 1383, 1266, 1228, and 1209 cm^{-1} can be

seen in both spectra (Table 2). Below 800 cm^{-1}, bands at 754 and 732 cm^{-1} were observed in the spectra obtained with normal abundance THF. The solution spectrum is somewhat noisier because of solvent subtraction.

Table 2. Infrared Spectroelectrochemistry of Iron Porphyrins

compound	ν_{CO} (cm^{-1})	ν_{NO} (cm^{-1})	other infrared bands/cm^{-1}	reference
Fe^{III}(OEPone)Cl	1719		1563, 1536, 1383, 1268, 1228, 1221, 1209, 754, 732	this work
Fe^{II}(OEPone)	1703		1550, 1530, 1361, 1221, 754, 742	this work
Fe(OEPone)$^-$	1671, 1578		1609, 1548, 1526, 1361, 1219, 728	this work
Cu^{II}(OEPone)	1710			36
Cu^{II}(OEPone)$^+$	1730			36
Ni^{II}(OEPone)	1711			37
Fe^{III}(OEPdione)Cl	1717		1580, 1560, 1543, 1526, 1294, 1270, 1243, 1221, 1217	this work
Fe^{II}(OEPdione)	1703		1547, 1524, 1380, 1361, 1220	this work
Fe(OEPdione)$^-$	1671, 1655, 1648, 1640		1593, 1562, 1535, 1265, 1240, 1219	this work
Fe(OEP)(NO)		1670	1460, 1377, 1317, 1273, 1223	this work
Fe(TPP)(NO)		1681a		28
Fe(OEP)(NO)$^-$		1441	1343, 1273, 1221	this work
Fe(TPP)(NO)$^-$		1496a		28
Fe(OEPone)(NO)	1715	1662	1682, 1560, 1541, 1242	this work
Fe(OEPone)(NO)$^-$	1702	1442	1674, 1579, 1547, 1484, 1466, 1262	this work
Fe(OEPdione)(NO)	1714	1665	1576, 1551, 1272	this work
Fe(OEPdione)(NO)$^-$	1691	1442	1570, 1265	this work

[a]By resonance Raman spectroscopy.

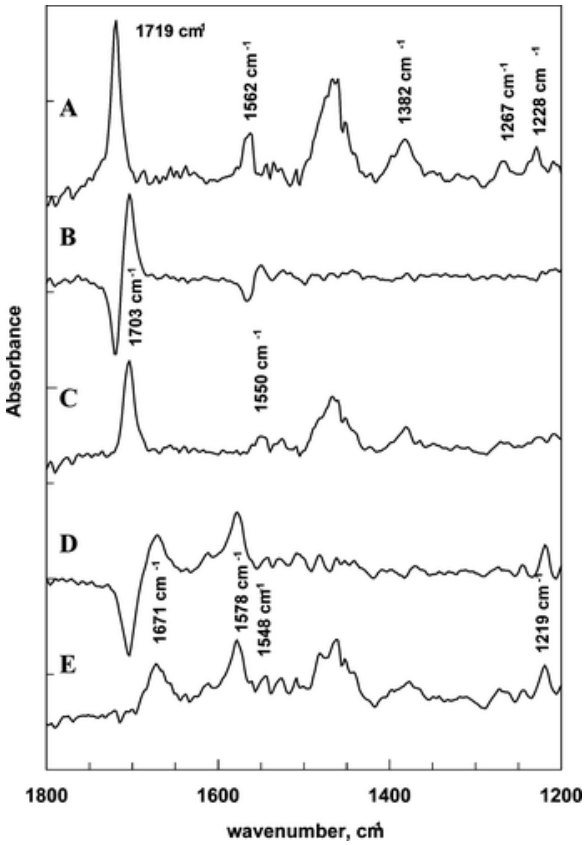

Figure 1. (A) FTIR spectrum of Fe(OEPone)Cl. (B) FTIR difference spectrum for Fe(OEPone) − Fe(OEPone)Cl. (C) FTIR spectrum of Fe(OEPone). (D) FTIR difference spectrum of $Fe(OEPone)^-$ − Fe(OEPone). (E) FTIR spectrum of $Fe(OEPone)^-$. Spectra A, C, and E are solvent subtracted. Solvent: THF-d_8; electrolyte: TBAP.

The first two reduction waves were examined by infrared spectroelectrochemistry. The FTIR spectra of Fe^{III}(OEPone)Cl, Fe^{II}(OEPone), and $Fe(OEPone)^-$ as well as their difference spectra are shown in Figure 1. For the first reduction, the most noticeable change that was observed was the shift in the carbonyl band from 1719 cm^{-1} shifted to 1703 cm^{-1}. This would indicate a weakening of the macrocycle carbonyl band, and is probably due to the increased electron density on the porphyrin ring because of back-bonding from the Fe(II) atom to the porphyrin. Another important feature of the ferrous complex was that the absorptivity of the carbonyl band was roughly the same in both the ferric and the ferrous complexes. In addition, there was a shift in the 1562 cm^{-1} band to 1550 cm^{-1}. DFT calculations, discussed below, indicated that this band is due to C_m-C_α and C_β-C_β vibrations. The band at 754 cm^{-1} was broader than a typical band and might be an overlap of two bands. Upon reduction one of the bands shifted to 742 cm^{-1}, but the 754 cm^{-1} is still present in the ferrous spectrum, but now appeared sharper. Outside of these vibrations, the ferrous and ferric porphinone spectra are similar.

Upon further reduction to the $Fe(OEPone)^-$ complex, the carbonyl band shifted to lower energy (1671 cm^{-1}), indicating a further weakening of the porphinone carbonyl group. A second strong new band appeared at 1578 cm^{-1}, as well as several new bands were observed at 1609, 1548, 1526, and 1219 cm^{-1}. The difference spectrum for $Fe(OEPone)^-$ − Fe(OEPone) is shown in Figure 1. Below 800 cm^{-1}, the band at 754 cm^{-1} decreased significantly upon the formation of the iron(I) species, and a shoulder at 775 cm^{-1} and a new band at 728 cm^{-1} were observed. The relationship between the 754 cm^{-1} band and the two new bands that were observed is not clear at this time. The results are summarized in Table 2.

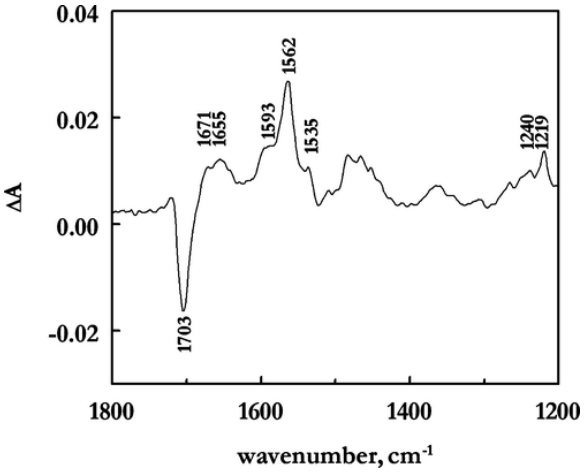

Figure 2. Difference spectrum of Fe(OEPdione)$^-$ minus Fe^{II}(OEPdione). Solvent: THF-d_8; electrolyte: 0.10 M TBAP.

Similar infrared spectroelectrochemical results were also observed for Fe(OEPdione)(Cl) (Table 2). In solution, Fe(OEPdione)Cl has a strong broad band at 1717 cm^{-1} due to the carbonyl vibration, which is split into two bands in a KBr pellet (1710 and 1720 cm^{-1}). As with Fe(OEPone)Cl, the initial reduction to the ferrous complex gave rise to a small shift in the carbonyl band (1717 to 1703 cm^{-1}). A single carbonyl band was observed in the ferrous complex, as was seen in the porphinone complex. The 1560 and 1580 cm^{-1} band disappeared, and a new band was observed at 1547 cm^{-1}, which was quite similar to the Fe(OEPone)Cl reduction. As with the porphinone complex, the reduction is known to be metal centered, but the ferrous complex can backbond to the porphyrin, which may be the source of these shifts. The difference spectrum for the reduction of Fe^{II}(OEPdione) to Fe(OEPdione)$^-$ is shown in Figure 2. The ν_{CO} band at 1703 cm^{-1} band decreased, as with the reduction of the Fe^{II}(OEPone) complex, and several new prominent bands were observed between 1671 and 1535 cm^{-1}. Unlike the ferrous and ferric complexes, the formal iron("I") complex had no single strong carbonyl band. This is due to the strong mixing of the carbonyl vibration with the porphyrin ring vibrations, as the carbonyl vibration moves to lower energy.

DFT calculations were performed on the iron(III) and iron("I") complexes, using octamethyl porphinones (OMPone and OMPdione, for the porphinone and porphinedione, respectively) as the macrocycle to minimize computational time. The ν_{CO} band in the calculated infrared spectrum of Fe^{III}(OMPdione)Cl compared well with the experimental spectrum for Fe^{III}(OEPdione)Cl with a single band (made up of two overlapping bands) at 1706 cm^{-1} (compared to 1717 cm^{-1} in solution). Upon reduction of the complex to the iron("I") complex, the C═O stretching internal coordinate became distributed over a number of normal modes, leading to additional features in the spectrum, with calculated frequencies of 1660, 1649, 1625, 1605, and 1585 cm^{-1}. This compares well to the observed frequencies of 1671, 1655, 1648, 1640, and 1593 cm^{-1} for Fe(OEPdione)$^-$. The distribution of the ν_{CO} mode into several bands in the formal iron("I") state led to a lower intensity of each band as compared to the ferrous complex. The highest occupied molecular orbital (HOMO), calculated by DFT for Fe(OMPdione)$^-$, is shown in Figure 3. The orbital shows considerable electron density on the macrocycle with relatively little in the iron d-orbital. The antibonding character of the C═O bond is consistent with the decrease in the ν_{CO} band upon reduction. While this orbital indicates both Fe(I) and π-radical anion character for the formal iron("I") complex, the latter structure better represents the Fe(OEPdione)$^-$ structure.

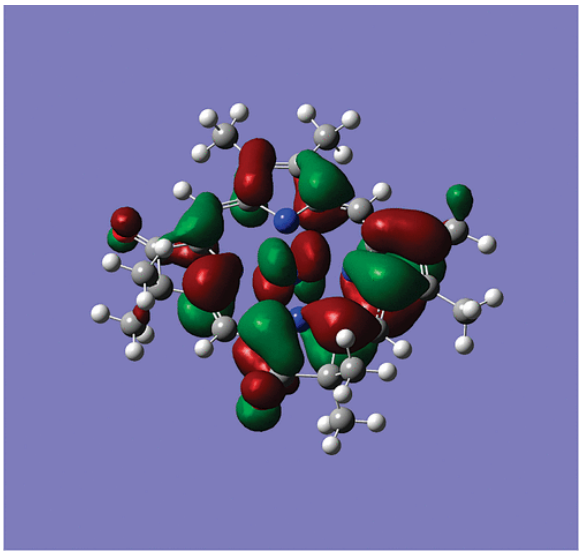

Figure 3. DFT calculated HOMO orbital for Fe(OMPdione)$^-$.

DFT calculations of Fe(OMPone)$^-$ indicated two bands with significant C═O stretching modes. These bands, 1672 and 1578 cm^{-1}, were also the strongest bands in the Fe(OEPone)$^-$ spectrum. The calculated frequencies were 1655 and 1585 cm^{-1}. Other observed (calculated) bands were seen at 1609 (1614), 1548 (1556), 1219 (1240), and 728 (734) cm^{-1}. The HOMO orbital for Fe(OMPone)$^-$ shows considerably more electron density on the central iron than was observed with the porphinedione macrocycle. More detailed study of the normal modes of the ferrous and "Fe(I)" porphinone complexes would be needed to verify this prediction.

Infrared Spectroelectrochemistry of Fe(P)(NO)

The thin-layer infrared spectroelectrochemistry of iron porphyrin nitrosyl complexes was also examined. The $E_{1/2}$ values for the nitrosyl complexes studied are summarized in Table 1. The spectra of Fe(OEP)(NO) and Fe(OEP)(NO)$^-$ are shown in Figure 4, along with the spectrum in a KBr pellet. As before, excellent correspondence was observed between the KBr and solution spectrum. The most prominent band was due to the nitrosyl stretch, which appears at 1670 cm^{-1}. The ethyl bands around 1317, 1377, and 1460 cm^{-1} can also be clearly seen in both spectra. Additional bands observed in both spectra are at 1376, 1316, 1273, and 1223 cm^{-1}.

The spectrum of the one-electron reduced product, Fe(OEP)(NO)$^-$, is also shown in Figure 4. The nitrosyl band at 1670 cm^{-1} disappeared and new bands at 1441 and 1343 cm^{-1} appeared. In addition, the bands at 1273 and 1221 cm^{-1} weakened, but did not disappear. The identity of the nitrosyl band for Fe(OEP)(NO)$^-$ was confirmed by the use of ^{15}N labeling of the nitrosyl. For Fe(OEP)(NO), only one isotope sensitive band was observed at 1670 cm^{-1} which, decreased to 1642 cm^{-1} upon ^{15}N isotopic substitution of the nitrosyl. For the reduction product, Fe(OEP)(NO)$^-$, the only isotopically sensitive band was the 1441 cm^{-1} band which downshifted to 1425 cm^{-1}. Both these shifts are consistent with the replacement of the ^{14}N isotope of nitrogen with ^{15}N. Reoxidation of Fe(OEP)(NO)$^-$ regenerated the original Fe(OEP)(NO) spectrum. In comparison with the Fe(TPP)(NO)$^-$ complex which has already studied by resonance Raman spectroscopy, (28) the decrease in the ν_{NO} for the OEP complex (231 cm^{-1}) is larger than the TPP complex (185 cm^{-1}) upon reduction, indicating less delocalization to the ring.

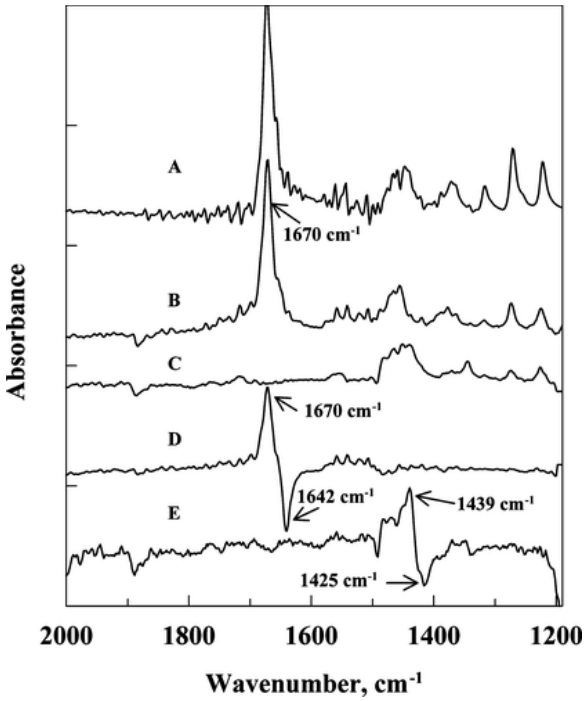

Figure 4. (A) FTIR spectrum of Fe(OEP)(NO) in KBr. (B) FTIR spectrum of Fe(OEP)(NO) in THF-d_8. (C) FTIR spectrum of Fe(OEP)$(NO)^-$ in THF-d_8. (D) Difference spectrum of Fe(OEP)(^{NA}NO) − Fe(OEP)(^{15}NO). (E) Difference spectrum of Fe(OEP)(^{NA}NO)$^-$ − Fe(OEP)(^{15}NO)$^-$. B/C solvent/electrolyte subtracted.

The spectroelectrochemistry of Fe(OEPdione)(NO) was examined next. Both the carbonyl and the nitrosyl vibrations were observed. In the starting complex, Fe(OEPdione)(NO), the ν_{CO} band was observed at 1714 cm^{-1} while the ν_{NO} band was at 1665 cm^{-1} (Figure 5, curve A). The ν_{CO} band was observed between the value for Fe^{III}(OEPdione)Cl (1718 cm^{-1}) and that for Fe^{II}(OEPdione) (1703 cm^{-1}). The ν_{NO} band at 1665 cm^{-1} was comparable to the same band in Fe(OEP)(NO) (1670 cm^{-1}). The spectrum obtained from the reduction of Fe(OEPdione)(NO) in d_8-THF is shown in Figure 5, curve C, and the difference spectrum in Figure 5, curve B. The most noticeable shifts are the bands at 1714 and 1665 cm^{-1}, which are due to ν_{CO} and ν_{NO}, respectively. The 1714 cm^{-1} shifted to 1691 cm^{-1} with a shoulder at 1681 cm^{-1}, while the 1665 cm^{-1} disappeared and a new band at 1442 cm^{-1} appeared, which is similar to the ν_{NO} band for Fe(OEP)$(NO)^-$. A series of bands between 1597 and 1622 cm^{-1} and also between 1483 and 1450 cm^{-1} appeared, and the 1576 cm^{-1} shifted to 1570 cm^{-1}. As with the previous complexes, reoxidation of Fe(OEPdione)$(NO)^-$ led to the regeneration of Fe(OEPdione)(NO), indicating that the reduced complex was stable on the experimental time scale.

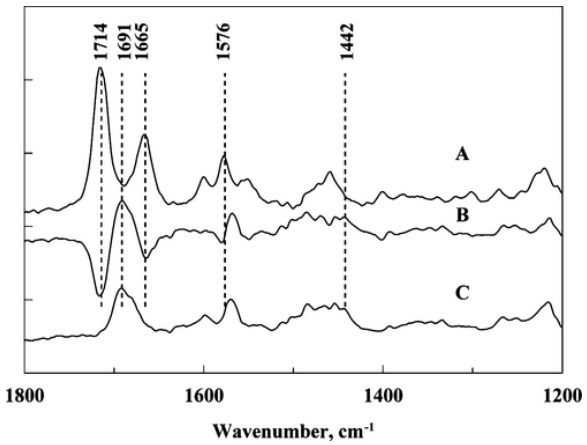

Figure 5. (A) FTIR spectrum of Fe(OEPdione)(NO). (B) Difference spectrum of $Fe(OEPdione)(NO)^-$ − Fe(OEPdione)(NO). (C) FTIR spectrum of $Fe(OEPdione)(NO)^-$. Solvent: THF-d_8; electrolyte: 0.10 M TBAP. Spectra A/C are solvent/electrolyte subtracted.

DFT calculations on Fe(OMPdione)(NO) and its reduced product were also carried out (as noted earlier, the methyl substituents were used in DFT calculations). The ν_{CO} and ν_{NO} bands in the starting materials were calculated to be 1703 and 1700 cm^{-1}, respectively. The observed values were found to be 1714 and 1665 cm^{-1}, while Praneeth et al. (38) calculated a ν_{NO} band at 1703 cm^{-1} for P = porphine. Upon reduction, the calculated decrease in the ν_{CO} band was 32 cm^{-1}, while the ν_{NO} band decreased by 154 cm^{-1}. This compares to the decreases observed in this work of 23 cm^{-1} and 223 cm^{-1}, respectively. For the $TFPPBr_6$ ligand used by Pellegrino et al., (7) a decrease of 166 cm^{-1} was observed. Similar decreases in the ν_{NO} band were calculated by Lehnert et al. (8) The HOMO orbital for $Fe(OMPdione)(NO)^-$ is shown in Figure 6. The electron density calculated for $Fe(OMPdione)(NO)^-$ is very similar to the HOMO calculated by Pellegrino et al., (7) reflecting a strong Fe-NO σ-bond between the doubly occupied π * orbital from NO and the empty d_z^2 iron orbital.

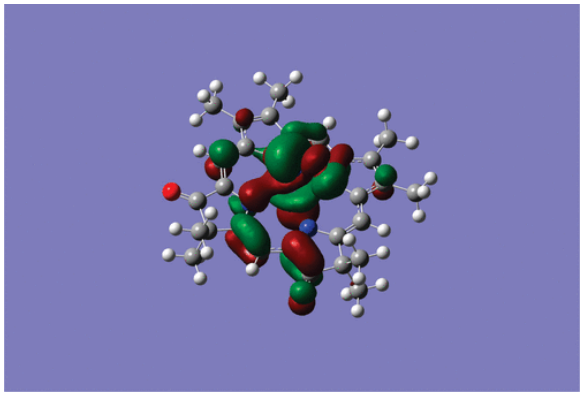

Figure 6. DFT calculated HOMO orbital for $Fe(OMPdione)(NO)^-$.

Part of the difficulty in calculating the ν_{NO} band in the $Fe(P)(NO)^-$ complex is the tendency of DFT calculations to "over-delocalize" an orbital. In this case, this has led to a larger calculated decrease in the carbonyl band, compared to experimental, and a smaller decrease in the nitrosyl band. This "over-delocalization" or "self-interaction error" (SIE) has been discussed by Cohen et al. for the dissociation of H_2^+. (39) Lundberg and Siegbahn (40) have also examined this issue for radicals and transition metal complexes, and have found that DFT will artificially stabilize delocalized states. The net effect of this is to allow too much electron density of the HOMO to appear on the porphine ligand (causing the ν_{CO} to decrease too much), and reduce the electron density on the Fe-NO moiety (causing the ν_{NO} to decrease too little). Similar problems may lead to the under-estimation of the Fe(I) character of $Fe(P)^-$ in DFT calculations.

The overall results that were observed for Fe(OEPone)(NO) were similar to the porphinedione complex for the ν_{NO} band. The spectra are shown in Figure 7. The ν_{NO} for Fe(OEPone)(NO) was 1662 cm^{-1}, which decreased to 1442 cm^{-1} upon reduction. The ν_{CO} at 1715 cm^{-1} decreased upon reduction, but several new bands were observed between 1670 and 1705 cm^{-1} (Table 2). A strong band was not observed in the 1550 cm^{-1} region as was seen for the $Fe(P)^-$ complexes. The spectrum in the ν_{NO} region was more congested than for the other complexes studied and the lack of a strong ν_{CO} may indicate that several new bands may occur because of coupling of various ring modes. Other observed changes were the shift in the 1682 cm^{-1} band to 1674 cm^{-1}, the disappearance of the 1560 and 1541 cm^{-1} band, new bands at 1579, 1547, 1484, and 1466 cm^{-1}, and an increase in the absorbance of the 1217 cm^{-1} band.

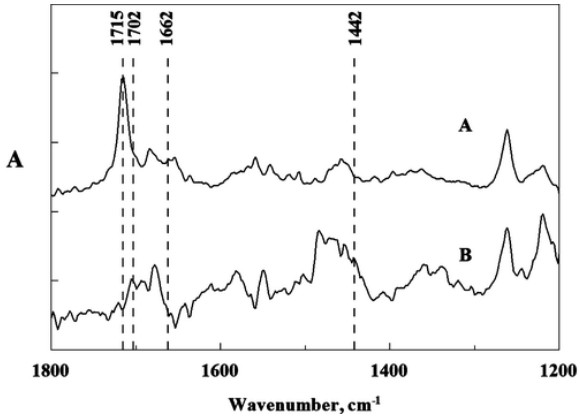

Figure 7. (A) FTIR spectrum of Fe(OEPone)(NO). (B) FTIR spectrum of Fe(OEPone)(NO)$^-$. Both Spectra are solvent/electrolyte subtracted. Solvent: THF-d_8; electrolyte: 0.10 M TBAP.

Conclusions

The reduction of iron in iron porphinones can be observed in changes in the carbonyl infrared band. When ferric porphinones were reduced to the ferrous complex, the ν_{CO} band decreased by 16 cm^{-1}. This downshift can be attributed to the increased back-bonding between the d_π orbitals of the metal with the porphinone orbital. Further reduction of the ferrous complex led to more complexity in the infrared spectra. Both experimental and DFT calculations show that the single infrared band in the ferrous complex is split into several bands in the reduced product. DFT calculations show that the carbonyl normal mode becomes more coupled with the ring vibrations when shifted to a lower energy. Taking the carbonyl band of highest energy, formation of the formal Fe(I) complex caused a further decrease of 32 cm^{-1} for both the porphinone and the porphinedione complexes when compared with the ferrous complex. This was twice the decrease of the predominantly metal centered ferric/ferrous reduction. The DFT calculation predicts that more electron density is on the porphinone ring with OMPdione as compared to OMPone. The highest vibration with C═O stretching component is the same for both ligands (1671 cm^{-1}) and might appear to contradict this. On the other hand, for the dione, the electron density is spread over two carbonyl groups, which is consistent with more density on the ring even with the same vibrational energy. As the carbonyl vibration is shifted to lower energy, significant coupling between the ring and the carbonyl modes was observed for both the Fe(P)(Cl) and the Fe(P)(NO) complexes.

For the nitrosyl complexes, there was a consistent downshift in the ν_{NO} band from about 1665 cm^{-1} to 1442 cm^{-1} for all three macrocycles. This indicates that the carbonyl groups on the porphine ring have little effect on the electron density in the Fe-NO moiety. This is consistent with the DFT calculations that showed considerably less delocalization of the HOMO to the porphinone ring, as compared to the "Fe(I)" complexes. The effect of the carbonyl group, as seen in Figure 6, is to change the distribution of the electron density on the ring from a relatively symmetrical distribution when P = porphine to an asymmetric distribution when P = porphinedione. The net electron density on the Fe-NO group is essentially unchanged (hence the ν_{NO} is unaffected). The ν_{CO} band (highest energy band) was also consistent with this interpretation. The ν_{CO} for Fe(OEPone)(NO)$^-$ and Fe(OEPdione)(NO)$^-$ were 1702 and 1691 cm^{-1}, respectively. These vibrations were considerably higher than the ν_{CO} for Fe(OEPone)$^-$ and Fe(OEPdione)$^-$ (1671 cm^{-1}), indicating considerably less delocalization of the added electron to the ring in the nitrosyl complex.

The use of FTIR spectroelectrochemistry in combination with DFT calculations was shown to be quite valuable in understanding the electronic structure of reduced iron porphinone complexes. The energy of the carbonyl vibration was quite sensitive to the interaction between the central metal and the porphinone ring. Work is in

progress in our laboratory to see whether these effects can also be monitored when other transition metals replace iron as the central metal.

References

1 Yamaguchi, K. and Morishima, I. Inorg. Chem. 1992, 31, 3216– 3222
2 Donohoe, R. J., Atamian, M., and Bocian, D. F. J. Am. Chem. Soc. 1987, 109, 5593– 5599
3 Liu, Y. M., DeSilva, C., and Ryan, M. D. Inorg. Chim. Acta 1997, 258, 247– 255
4 Liu, Y. and Ryan, M. D. Inorg. Chim. Acta 1994, 225, 57– 66
5 Chang, C. K., Barkigia, K. M., Hanson, L. K., and Fajer, J. J. Am. Chem. Soc. 1986, 108, 1352– 1354
6 Liu, Y. M., DeSilva, C., and Ryan, M. D. Inorg. Chim. Acta 1997, 258, 247– 255
7 Pellegrino, J., Bari, S. E., Bikiel, D. E., and Doctorovich, F. J. Am. Chem. Soc. 2009, 132, 989– 995
8 Lehnert, N., Praneeth, V. K. K., and Paulat, F. J. Comput. Chem. 2006, 27, 1338– 1351
9 Kadish, K. M., Mu, X. H., and Lin, X. Q. Inorg. Chem. 1988, 27, 1489– 1492
10 Mu, X. H. and Kadish, K. M. Inorg. Chem. 1988, 27, 4720– 4725
11 Mu, X. H. and Kadish, K. M. Langmuir 1990, 6, 51– 56
12 Hu, Y., Han, B. C., Bao, L. Y., Mu, X. H., and Kadish, K. M. Inorg. Chem. 1991, 30, 2444– 2446
13 Hinman, A. S., Pavelich, B. J., Kondo, A. E., and Pons, S. J. Electroanal. Chem. 1987, 234, 145– 162
14 Hinman, A. S., Pavelich, B. J., and McGarty, K. Can. J. Chem. 1988, 66, 1589– 1595
15 Jones, D. H. and Hinman, A. S. J. Chem. Soc., Dalton Trans. 1992, 1503– 1508
16 Zheng, G. D., Stradiotto, M., and Li, L. J. J. Electroanal. Chem. 1998, 453, 79– 88
17 Kincaid, J. R., Urban, M. W., Watanabe, T., and Nakamoto, K. J. Phys. Chem. 1983, 87, 3096– 3101
18 Li, X.-Y., Czernuszewicz, R. S., Kincaid, J. R., Stein, P., and Spiro, T. G. J. Phys. Chem. 1990, 94, 47– 61
19 Ogoshi, H., Masai, N., Yoshida, Z., Takemoto, J., and Nakamoto, K. Bull. Chem. Soc. Jpn. 1971, 44, 49– 51
20 Paulat, F., Praneeth, V. K. K., Nather, C., and Lehnert, N. Inorg. Chem. 2006, 45, 2835– 2856
21 Prendergast, K. and Spiro, T. G. J. Phys. Chem. 1991, 95, 1555– 1563
22 Mylrajan, M., Andersson, L. A., Loehr, T. M., Wu, W., and Chang, C. K. J. Am. Chem. Soc. 1991, 113, 5000– 5005
23 Kini, A. D., Washington, J., Kubiak, C. P., and Morimoto, B. H. Inorg. Chem. 1996, 35, 6904– 6906
24 Moss, D., Nabedryk, E., Breton, J., and Mäntele, W. Eur. J. Biochem. 1990, 187, 565– 572
25 Teraoka, J., Hashimoto, S., Sugimoto, H., Mori, M., and Kitagawa, T. J. Am. Chem. Soc. 1987, 109, 180– 184
26 Mashiko, T., Reed, C. A., Haller, K. J., and Scheidt, W. R. Inorg. Chem. 1984, 23, 3192– 3196
27 Hickman, D. L., Shirazi, A., and Goff, H. M. Inorg. Chem. 1985, 24, 563– 566
28 Choi, I.-K., Liu, Y., Feng, D., Paeng, K. J., and Ryan, M. D. Inorg. Chem. 1991, 30, 1832– 1839
29 Chang, C. K. and Sotiriou, C. J. Org. Chem. 1985, 50, 4989– 4991
30 Chang, C. K., Sotiriou, C., and Wu, W. J. Chem. Soc., Chem. Commun. 1986, 1213– 1215
31 Richardson, P. F., Chang, C. K., Hanson, L. K., Spaulding, L. D., and Fajer, J., J. Phys. Chem. 1979, 83, 3420– 3424
32 Lin, X. Q. and Kadish, K. M. Anal. Chem. 1985, 57, 1498– 1501
33 Krejcik, M., Danek, M., and Hartl, F. J. Electroanal. Chem. 1991, 317 (1–2) 179– 187
34 Frisch, M. J., Trucks, G. W., Schlegel, H. B., Scuseria, G. E., Robb, M. A., Cheeseman, J. R., Montgomery, J. A., Jr., Vren, T., Kudin, K. N., Burant, J. C., Millam, J. M., Iyengar, S. S., Tomasi, J., Barone, V., Mennucci, M., Cossi, M., Scalmani, G. N., Rega, N., Petersson, G. A., Nakatsuji, H., Hada, M., Ehara, M., Toyota, K., Fukuda, R., Hasegawa, J., Ishida, M., Nakajima, T., Honda, Y., Kitao, O., Nakai, H., Klene, M., Li, X., Knox, J. E., Hratchian, H. P., Cross, J. B., Adamo, C., Jaramillo, J., Gomperts, R., Stratmann, R. E., Yazyev, O., Austin, A. J., Cammi, R., Pomelli, C., Ochterski, J. W., Ayala, P. Y., Morokuma, K., Voth, G. A., Salvador, P., Dannenberg, J. J., Zakrzewski, V. G., Dapprich, S., Daniels, A. D., Strain, M. C., Farkas, O., Malick, D. K., Rabuck, A. D., Raghavachari, K., Foresman, J. B., Ortiz, V. J., Cui, Q., Baboul, A. G., Clifford, S., Cioslowski, J., Stefanov, B. B., Liu, G., Liashenko, A., Piskorz, P., Komaromi, I., Martin, R. L., Fox, D. J., Keith, T., Al-Laham, M. A., Peng, C. Y., Nanayakkara, A., Challacombe, M., Gill, P. M. W., Johnson, B., Chen, W.,

Wong, M. W., Gonzalez, C., and Pople, J. A. Gaussian 03, Revision C.02; Gaussian,Inc.: Wallingford, CT, 2004.
35 Wachters, A. J. H. J. Chem. Phys. 1970, 52, 1033– 1036
36 Neal, T. J., Kang, S. J., Schulz, C. E., and Scheidt, W. R. Inorg. Chem. 1999, 38, 4294– 4302
37 Stolzenberg, A. M., Glazer, P. A., and Foxman, B. M. Inorg. Chem. 1986, 25, 983– 991
38 Praneeth, V. K. K., Nather, C., Peters, G., and Lehnert, N. Inorg. Chem. 2006, 45, 2795– 2811
39 Cohen, A. J., Mori-Sanchez, P., and Yang, W. Science 2008, 321, 792– 794
40 Lundberg, M. and Siegbahn, P. E. M. J. Chem. Phys. 2005, 122, 224103−1– 224103/9